Chinese Science Bulletin 2003 Vol. 48 No. 23 2549—2561

Evolution of the South China Sea and monsoon history revealed in deep-sea records

WANG Pinxian[1], JIAN Zhimin[1], ZHAO Quanhong[1], LI Qianyu[1], WANG Rujian[1], LIU Zhifei[1], WU Guoxuan[1], SHAO Lei[1], WANG Jiliang[1], HUANG Baoqi[1], FANG Dianyong[1], TIAN Jun[1], LI Jianru[1], LI Xianhua[2], WEI Gangjian[2], SUN Xiangjun[3], LUO Yunli[3], SU Xin[4], MAO Shaozhi[4] & CHEN Muhong[5]

1. Laboratory of Marine Geology, MOE, Tongji University, Shanghai 200092, China;
2. Guangzhou Institute of Geochemistry, Chinese Academy of Sciences, Guangzhou 510640, China;
3. Institute of Botany, Chinese Academy of Sciences, Beijing 100093, China;
4. China University of Geosciences, Beijing 100083, China;
5. South China Sea Institute of Oceanology, Chinese Academy of Sciences, Guangzhou 510301, China

Abstract **As the third summary report of ODP Leg 184 to the South China Sea (SCS), this paper discusses the evolution of the East Asian monsoon and the SCS basin. A multi-proxy approach, involving geochemistry, micropaleontology, pollen and other analyses, was adopted for reconstructing the evolutionary history of the East Asian monsoon, which was characterized by a series of paleo-climate events especially at 8, 3.2, 2.2 and 0.4 Ma. The new record indicates similar stages in the development of the East and South Asian monsoons, with an enhanced winter monsoon over East Asia being the major difference. The rich spectrums of monsoon variability from the southern SCS also reveal other characteristic features of the low latitude ocean. Evidence for the evolution of the SCS includes the hemipelagic Oligocene sediments, implying the existence of deep water environments during the early seafloor spreading stage of the SCS basin. The four major unconformities and some remarkable diagenetic features in upper Oligocene deposits indicate the strongest tectonic events in the region. From a careful comparison of lithologies and sedimentation rates, we conclude that the prominent differences in sedimentary environments between the southern and northern SCS were established only by ~3 Ma.**

Keywords: ODP Leg 184, South China Sea, deep-sea deposition, East Asian monsoon, basin evolution.

DOI: 10.1360/03wd0156

Ocean Drilling Program Leg 184 to the South China Sea in the spring of 1999 was a breakthrough for deep-sea research off China, and the follow-up laboratory studies have generated significant paleo-environmental results. In the first and second summary reports[1,2], we introduced the establishment of the best deep-sea stratigraphic sections in the west Pacific, and discussed the role of tropical carbon cycling in the evolution of climate periodicity. All these address global issues based on the SCS data, yet the main subject of ODP Leg 184 was the "East Asian monsoon history as recorded in the South China Sea and its global climate impact". The present paper, therefore, will focus on the sediment records of the East Asian monsoon evolution and of the opening history of the SCS basin, as well as the succeeding changes in depositional environments.

Paleomonsoon studies started over 20 years ago in the Indian Ocean, in particular ODP legs to the Arabian Sea have provided the best records of the South Asian monsoon[3]. The subsequent studies on the East Asian monsoon were most successful using terrestrial records from the Chinese Loess Plateau, and propagated later to studies offshore with emphases laid on the South China Sea. The German-Chinese collaborative project "Monitor-Monsoon" with SONNE-95 cruise in 1994 for the first time recovered high-quality, late Quaternary sediments from the SCS[4]; and ODP Leg 184 in 1999 cored continuous late Cenozoic sequences there[5], making the SCS a marine base for studying East Asian monsoons.

The geological explorations and scientific surveys in the SCS over the past 2—3 decades have accumulated a wealth of data bearing information on the evolution of its deep-sea basin. However, the geohistory of the SCS basin previously known was relied mostly on geophysical data, and numerous petroleum drill holes from the continental shelves yielded limited information on its evolution as a deep-sea basin. The Oligocene and younger deep-sea sediment sequence recovered from the lowermost northern continental slope during Leg 184 has provided the first direct evidence for the formation and development of the SCS deep water basin.

Therefor, two topics—the East Asian monsoon and SCS basin evolution—will be discussed successively in this paper on the basis of the Leg 184 results. Since there will be specific papers devoted to specific subjects, and since many analyses are still ongoing, we will limit ourselves here to a brief review of the progress. For the location of the drilling sites under discussion, see Fig. 1 and Table 1 in our first summary report "Thirty Million Year Deep-Sea Records in the South China Sea"[1].

1 Deep sea records of monsoon evolution

(i) Long term evolution. The main objects of ODP Leg 184 include (1) establishment of time series of monsoonal evolution, (2) extrapolation of its internal and external driving forces, and (3) comparison of the evolutionary history between the East and South Asian monsoons. The previous monsoon studies in the SCS were limited to the late Quaternary[6,7], and only ODP Leg 184 makes possible studies of the long-term monsoon evolution.

In terms of the long-term evolution, the first question

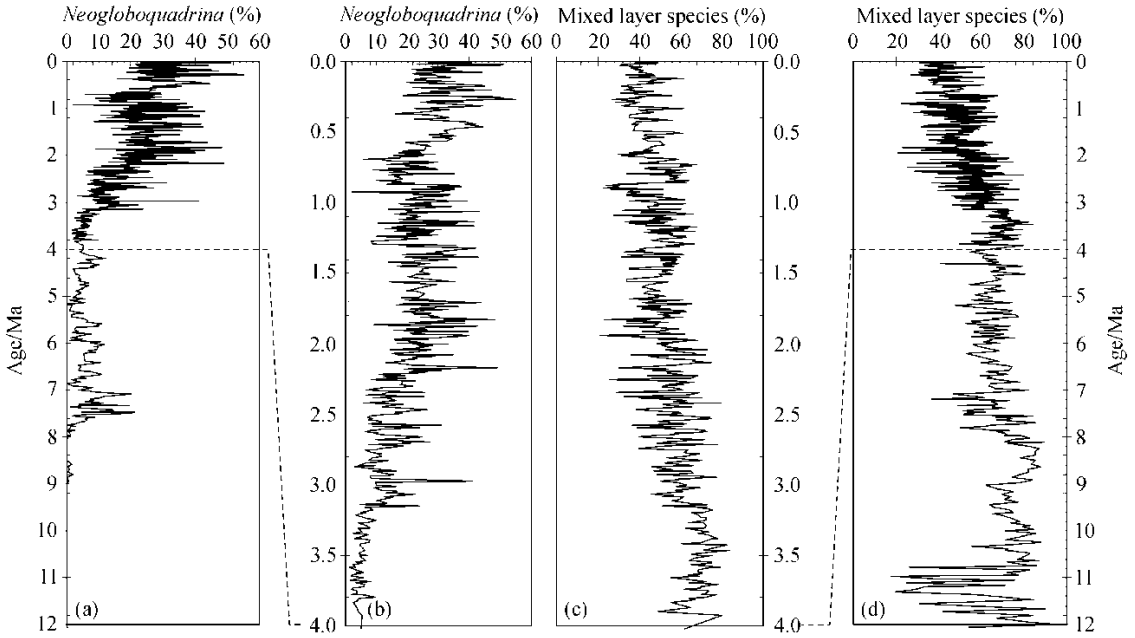

Fig. 1. Downcore variations of planktonic foraminifers% at Site 1146 since 12 Ma. (a) and (b) *Neogloboquadrina dutertrei*%; (c) and (d) percentage of the mixed layer shallow water species.

is to answer how old the East Asian monsoon history can be traced back. So far, the loess-paleosol profile spanning the last 2.6 million years provides the most intact record of the East Asian monsoon. With the study of the underlying Red Clay, the history of the monsoon has been extended to 7 to 8 Ma[8−10]. However, the recent discovery of the Miocene loess-paleosol profile at Qin'an, western Loess Plateau, implied that the East Asian monsoon could be traced back to 22 Ma at the least[11]. There is yet no deep-sea data to discuss the East Asian monsoon history over the entire late Cenozoic because pollen records from SCS sites are limited only to the Oligocene and the Quaternary. Therefore, we compiled available marine records from the South and East China Seas together with profiles from onshore basins of China to approach the Cenozoic evolution of the East Asian monsoon. From 120 off- and on-shore sites with pollen and paleobotanical data collected, plus lithological indicators from over the country, the distribution patterns of arid versus humid climates were reconstructed for five Cenozoic epochs. The results support the notion that a broad arid zone was stretching across China in the Paleogene, but retreated to the northwest by the end of the Oligocene, indicating the transition from a planetary to a monsoonal system in atmospheric circulation over the region[12−14]. A variety of evidence, such as the Qin'an Miocene loess profile[11], the monsoonal Miocene fauna discovered in southeast Asia[15], and paleo-climate modeling[16,17], all support the existence of the Asian monsoon in times no later than the early Miocene. At Site 1148, a series of element ratios such as Al/Ti, Al/K, Rb/Sr and La/L, indicative of the intensity of chemical weathering, increased abruptly around 29.5 Ma, in an early seafloor spreading stage of the SCS. This event implies an increase in humidity, although whether it was related to the first East Asian monsoon requires further examination.

In oceans, the monsoon-driven upwelling can lead to increased productivity and a shoaled thermocline. Important faunal signals of strengthened monsoons include abundance increases in productivity-indicative planktonic foraminifers due to upwelling, and decreases in the percentage of planktonic foraminifers living in the mixed layer because of a shoaled thermocline. The relative abundance of *Globigerina bulloides* is a good proxy of upwelling-related high productivity in the Arabian Sea[18], but it never shows high abundance in the SCS. Instead, the percentage changes of *Neogloboquadrina dutertrei* better unveil the monsoonal variability[19]. According to previous studies and comparison of various stable isotope measurements, species of *Globigerinoides*, *Globigerinita*, and *Globigerina* comprise the major part of shallow water dwellers in the mixed layer. Fig. 1 plots the variability of *N. dutertrei* % and shallow water dwellers % at Site 1146 in the northern SCS over the past 12 million years. From this figure we can find that *N. dutertrei* % abruptly increased at 7.6 Ma, and further increased from 3.2 Ma to 2.0 Ma; similarly, the shallow water dwellers % decreased abruptly after 8 Ma and further decreased from 3.2 Ma to 2.0 Ma, coincident with the trend of *N.*

dutertrei %, although the curve of shallow water dwellers % is distorted by carbonate dissolution around 11 Ma. Together, these planktonic foraminiferal results indicate paleomonsoon enhancements at 8—7 Ma and 3.2—2 Ma. A strengthening of the summer monsoon around 8 Ma is also supported by the increase in Pyloniid radiolarians at Site 1143. Considering the first obvious strengthening of the Indian monsoon at 8 Ma[3,20] broadly concurred with the initiation of the Red Clay eolian deposition on the loess plateau[8,21], the SCS results confirm a significant enhancement of the Asian monsoon system around 8 Ma[10,22]. Further development of monsoons from 3.2 Ma to 2.0 Ma was also manifested by the increase of opal abundance at Site 1143 [23] and by drastic coarsening of terrigenous clastic grain size due to intensified eolian transportation. Judging from the modern planktonic foraminiferal δ^{13}C distribution pattern in the region, the prominent decrease in planktonic δ^{13}C at Site 1148 from 3.1 Ma to 2.2 Ma likely has responded to the intensification of the winter monsoon[24]. In the modern SCS, winter monsoons exert a major influence on the variations of productivity and thermocline depth. Therefore, the Leg 184 monsoonal proxies discussed above are interpreted as resulted from the intensification of the winter monsoon caused by the growth of boreal ice sheets.

(ii) Orbital cycles. As a tropical process, the summer monsoon is primarily controlled by the precession[25], the amplitude of which is in turn controlled by the two eccentricity cycles, the 100 ka and 400 ka cycles. The procession cyclicity is the most distinct in the monsoonal records from the Mediterranean Sea[26], and occurs also in the SCS. Geochemical analyses of the 3.2—2.5 Ma sediments from Site 1145 in the northern SCS show obvious fluctuations of the K/Si ratio with the precession and eccentricity. The K/Si ratio represents the proportion of fluvial input in total sediments, and its fluctuations reveal the variations of summer-monsoon-induced precipitation (Fig. 2(c))[27] and, accordingly, the relationship between the summer monsoon and the orbital forcing. The most noticeable in Fig. 2(a) and (b) is the change of the 400 ka eccentricity cycle between 2.8 Ma and 3.2 Ma. Just at these two time points, the eccentricity and precession forcings were in their lowest values, presumably resulting in a weakened summer monsoon. Concomitantly, the foraminiferal δ^{13}C reached its heaviest values (Fig. 2(d), δ^{13}Cmax), implying that the ocean carbon reservoir had cyclic changes corresponding to the longer eccentricity cycle[28]. The relationship between monsoons and long carbon cycles has already been discussed in our second summary report[2], and the point to be made here is that the 400-ka-long eccentricity cycle observed in the Mediterranean monsoon records does exist also in the Asian monsoon system as recorded in the SCS.

Moving into the Quaternary with the growth of the boreal ice sheet, the monsoon circulation over the SCS has been tied more closely with glacial cycles, and the role of the winter monsoon strengthened further, as evidenced by the clay mineral and pollen records. Modern illite and chlorite in the SCS mainly come from the mainland of China and Taiwan Island, whereas smectite largely originates from the Luzon and islands of the southern SCS[30]. Therefore, the ratio of smectite versus illite+chlorite can be used to estimate the relative strength of the summer versus winter monsoons. This ratio was found to vary with glacial-interglacial cycles in the past 2 million years (Ma) at Site 1146: high values imply strong summer monsoons during interglacials, and low values imply strong winter monsoons during glacials. Furthermore, the fluctuation amplitude of this ratio decreased substantially over the past 0.4 Ma, suggesting a very strong winter monsoon even during the most recent interglacials (Fig. 3(b)). Vegetation has been more sensitive to monsoon influence. Previous pollen analyses already indicate that the winter monsoon strengthened while the summer monsoon weakened during the Last Glacial Maximum (LGM), resulting in the arid climate and the substitution of monsoon forest by grasslands to the northern SCS[31]. High-resolution pollen analyses from Site 1144 show herbs % and charcoal from natural fires increased during glacials and fern % that favored humid conditions increased during interglacials, indicating the cyclic changes of monsoons corresponding to glacial cycles have persisted throughout the whole record of the past one million years at this site[33]. Compared with all previous glacial records, the continuous increase in herbs and charcoal at Site 1144 implies a gradual strengthening trend of the winter monsoon toward the LGM.

The use of clay minerals and pollen from a deep-sea basin as monsoon proxies may be ambiguous because they are exotic grains transported from outside of the basin. Any rise or drop in sea level, any submergence or emergence of the shelf could disturb the records through re-deposition or other processes. A more direct proxy is the creatures living in the sea water. Fig. 4 shows the abundance variations of calcareous nannofossils and opal (mainly diatoms and radiolarians) for the past 1.6 Ma at Site 1143. Although the calcareous and siliceous fossils in the deep-sea sediments can be subject to dissolution, their accumulation rates increased during interglacials and decreased during glacials (Fig. 4(c), (d))[34,35], suggesting strong upwelling and high productivity induced by a strengthened summer monsoon during interglacials in the southern SCS. In contrast, at Site 1146 in the northern SCS, the opal abundance increased during glacials, likely as a result of winter monsoon induced upwelling.

Moreover, the stable isotopes are also useful proxies of monsoon induced upwelling. Evidence has shown that planktonic δ^{13}C is indicative of upwelling controlled

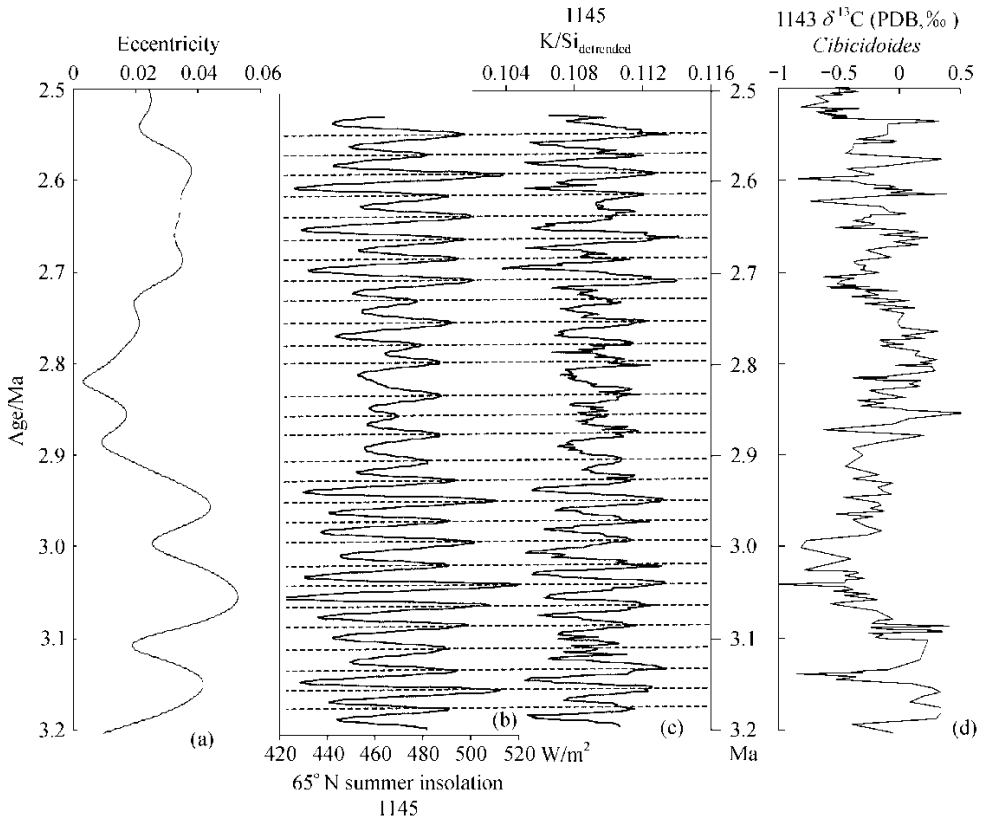

Fig. 2. Orbital forcing of the summer monsoon variations in the SCS in the late Pliocene (3.2—2.5 Ma). (a) Eccentricity[29]; (b) summer insolation at 65°N; (c) K/Si ratios at Site 1145[27]; (d) benthic δ^{13}C at Site 1143.

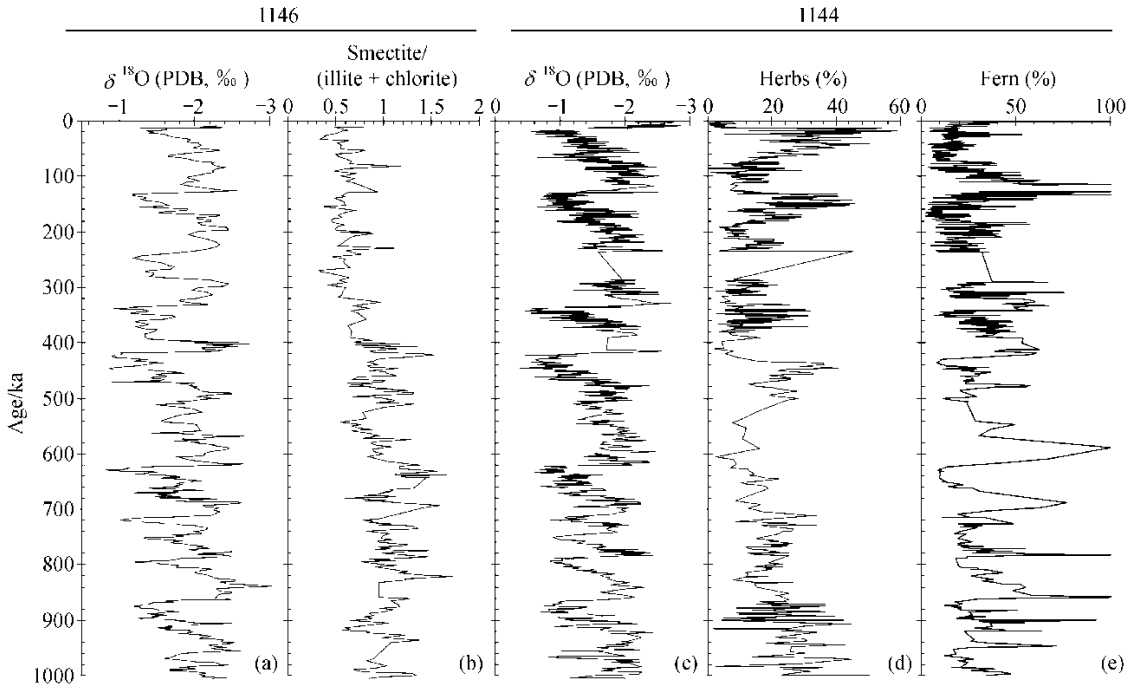

Fig. 3. Variations of monsoon proxies in the northern SCS in the last one million years. Site 1146: (a) planktonic δ^{18}O; (b) ratio of smectite/(illite+chlorite); Site 1144: (c) planktonic δ^{18}O; (d) herbs%; (e) ferns% (percentages in the total pollen sum).

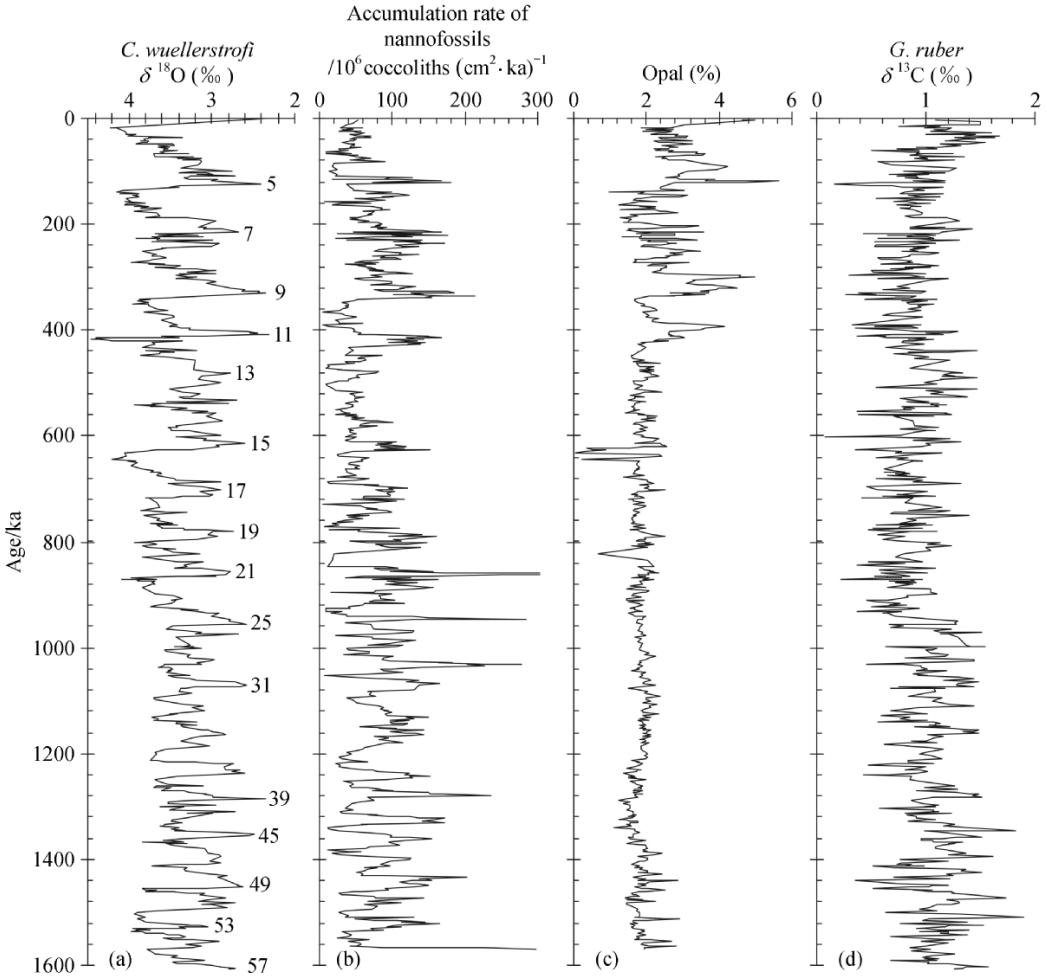

Fig. 4. Variations of monsoon proxies at Site 1143 in the southern SCS since 1.6 Ma. (a) Benthic δ^{18}O; (b) accumulation rate of nannofossils[34]; (c) opal%[35]; (d) planktonic *Globigerinoides ruber* δ^{13}C[28].

nutrient level in the SCS[7]; and that the δ^{18}O difference between mixed layer and thermocline species of planktonic foraminifers can be used to estimate thermocline depth in oceans[18,36]. The 1.6 Ma record of δ^{13}C difference between *Globigerinoides ruber,* a mixed layer species, and *Pulleniatina obliquiloculata,* a thermocline dweller from Site 1143 reveals the richest spectrum of orbital cycles including 100 ka, 40 ka and 20 ka, as well as the semi-precession cycle of 10 ka. Especially, the δ^{13}C difference is highly coherent with solar insolation at the precession band in the tropical climate regime. In sum, the monsoon records from deep-sea sediments of the southern SCS display a full range of periodicities, ranging from the 400 ka and 100 ka eccentricity cycles to the 40 ka obliquity cycle, the 20 ka precession cycle and the 10 ka semi-precession cycle, together as the characteristic of climate response in low latitude seas to the orbital forcing[37].

(iii) Discussion. For the first time ODP Leg 184 provides continuous marine records of the East Asian monsoon with a variety of time resolution. A comparison between these marine records and terrestrial records from loess sequences further confirms their comparability in probing into the integrity of the Asian monsoon system. In the Earth system perspective, the low latitude African, Asian and Australian monsoons comprise the bulk of the global monsoon system, all responding to orbital forcing in a way specific to low latitudes, with a characteristic wide range of periodicity ranging from the 400 ka eccentricity cycle to 10 ka semi-precession cycle. Meanwhile, the global monsoon system has sustained spatial and temporal variability on various timescales. From the ice-free early Cenozoic to the bi-polar ice-capped Quaternary, the response of the monsoon system to the solar insolation has become progressively complex. From Africa to East Asia, the complexity in land-sea distribution and topography increases eastward, and this geomorphological complexity furnished a more complicated East Asian monsoon system

as compared to the African monsoon. The East Asian monsoon excels the African monsoon not only by a wider meridian coverage but also by more complicated affecting factors. The East Asian monsoon system is influenced by cross-equatorial tropical forcing and some tropical-subtropical climate factors over the west Pacific and the Tibetan Plateau[38]. Therefore, the cyclicity of the East Asian monsoon variations has responded not only to tropical forcing but also to glacial forcing.

Judging from the modern process and Quaternary records, the effects of the winter monsoon appear to surpass that of the summer monsoon in the SCS. The low latitude precession forcing has nevertheless played a significant role in the local climate change even in the late Quaternary with very strong glacial forcing. For example, herbs % is coherent with foraminiferal $\delta^{18}O$ at Site 1144 (Fig. 4(d)) over the 100 ka eccentricity band, indicating the control by the waning and waxing of ice sheets, whereas its coherence with the Sun's insolation only at the precession band may indicate the precession forcing of the local climate. Another example is from the turn of Marine Isotope Stage (MIS) 6 to 5, at the beginning of the last interglacial, when the local vegetation change preceded the ice sheet change, implying a lead of climate changes in low and mid latitudes over high latitudes. All these examples highlight the importance of the tropical process in regional monsoon variations. The monsoon variability as a tropical process has its own cyclicity in low and mid latitudes, with weak responses to high latitude forcing during glacial cycles. As stated previously[2], the tropical process through carbon cycling modulates the global glacial cycles even under an "ice house" regime; the low latitude monsoon forcing coupled with a high latitude glacial forcing appears to have been the main control of climate change on Earth.

2 Major events in South China Sea evolution

(ⅰ) Deep-water Oligocene. The 32-Ma deep-sea record obtained during ODP Leg 184 not only provides a basis for exploring the global and regional climate evolution but also an archive of the SCS history. Of particular importance is the record involving the early development stage of the SCS found at Site 1148.

One of the outstanding contributions of the drilling is the discovery of deep-water Oligocene deposits, which indicate the existence of a deep-sea gulf prior to seafloor spreading in the SCS. The Oligocene/Miocene boundary at Site 1148 is marked by the first occurrence of *Paragloborotalia kugleri* (23.8 Ma) and the last occurrence of *Reticulofenestra bisectus* (23.9 Ma) at about the depth of 460 m (meter composite depth or mcd, as also below). The almost 400-m-thick section from below, between 859.45 m and 460 m, represents the 9 Ma long Oligocene between 32.8 Ma and 23.9 Ma, with the lower and upper Oligocene boundary (28.5 Ma) at about 488 m (see Table 3 in our first summary report[1]). Sediments of Oligocene age are mainly nannofossil-rich clay, containing deep-water trace fossils such as *Zoophycus*. The $CaCO_3$% averages from 30% to 60%, with much higher percentages in the upper than the lower Oligocene (Fig. 5(d)). Foraminiferal assemblage is predominated by planktonic species, with rare to common deep water benthic species such as the calcareous *Cibicidoides* and various agglutinated species, which comprise nearly 50% of the total foraminiferal biofacies in the early Oligocene[39]. Ostracods are characterized by deep-water species including *Krithe* with 30% to 40% abundance. These foraminiferal and ostracod assemblages indicates deep-water environments up to 1500 m, corresponding to the modern upper to middle continental slope, already existed in the Oligocene before seafloor spreading. The Oligocene sediment at Site 1148 is also enriched with pollen and nearshore phytoplankton, and its organic carbon content (0.4%—0.6%) is significantly higher than in the Neogene (<0.2%) (Fig. 5(c),(e),(f)), inferring a nearshore environment. Therefore, the very early Oligocene SCS must have been a narrow gulf with fairly steep slopes that facilitated the rapid accumulation of the thick lower Oligocene section between 859.45 m and 488 m at Site 1148.

The Oligocene SCS experienced a number of prominent environmental events. Noteworthy is the occurrence of thin-layered sandstones close to the base of the drilling holes at Site 1148, at a level with turbidite-associated agglutinated foraminifers[39] and with accumulation rates as high as 60 $g \cdot cm^{-2} \cdot ka^{-1}$ in a stage of rapid sedimentation. Of particular interest is the clear reflector at about 710 m in the seismic profile corresponding to a low-value trough in the $\delta^{13}C$ record from bulk sediment samples (Fig. 5(b)). At about the same depth, the proportion of fresh-water phytoplankton increases (Fig. 5(g)), and pollen assemblages show the replacement of tropical and subtropical low mountain and lowland evergreen vegetation by a temperate forest characterized by high mountain conifer and deciduous broadleaf trees, marking a drop in air temperature. All these may have responded to a major marine regression in the early Oligocene[40]. In the later part of the early Oligocene, the abundance of diatoms and radiolarian increased remarkably from 475 m to 600 m at Site 1148 (Fig. 5(h), (i)), similar to the record from the equatorial Pacific[41]. This increase of siliceous microfossils can be attributed to the fractionation in water chemistry between the Pacific and the Atlantic.

The whole late Oligocene deposition at Site 1148 belongs to slumping during 28.5—23.8 Ma, and the 28 m section between 488 m and 460 m (Fig. 6(a), unit VI) contains four unconformities: respectively at 488 m (28.5 Ma to 27.8 Ma missing), 478 m (27 Ma to 26 Ma),

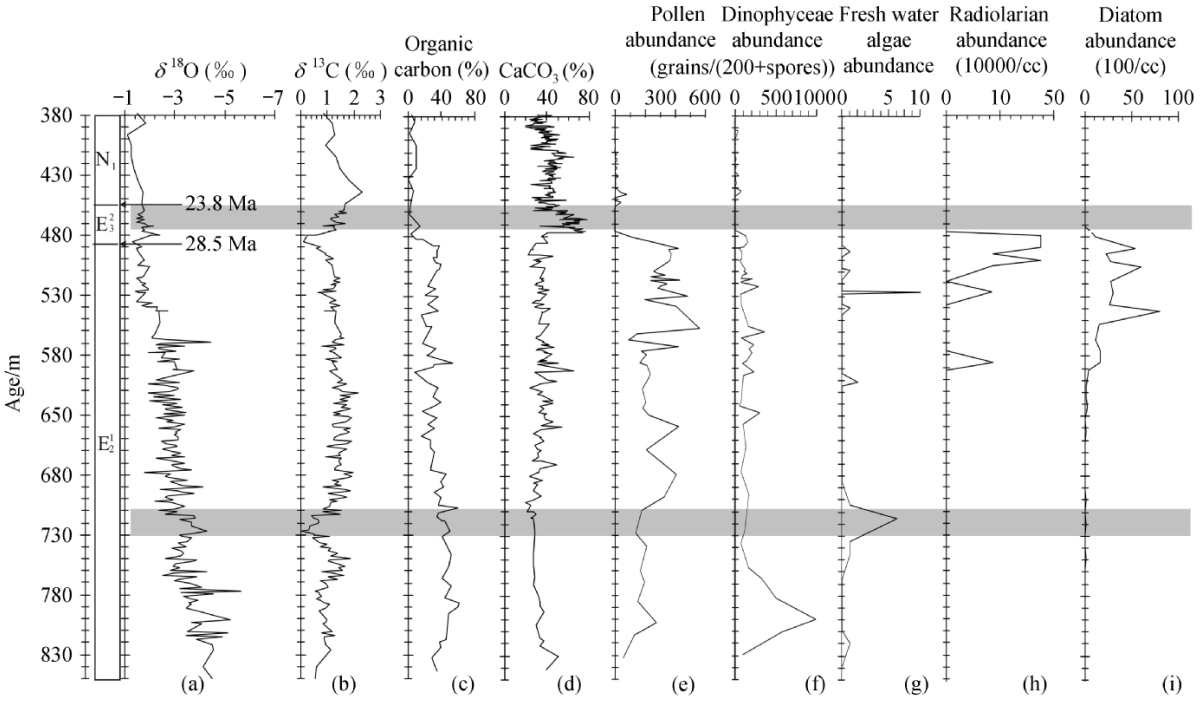

Fig. 5. Oligocene geochemistry and paleontology at Site 1148. (a) Bulk $\delta^{18}O$; (b) bulk $\delta^{13}C$; (c) C_{org} %; (d) $CaCO_3$%; (e) pollen abundance [grains/(200 exotic *Lycopodium* spores)]; (f) dinoflagellate abundance; (g) fresh water algae: *Pediastrum*, *Botryoccus* and *Concentricystis*; (h) radiolarian abundance (100/cc); (i) diatom abundance.

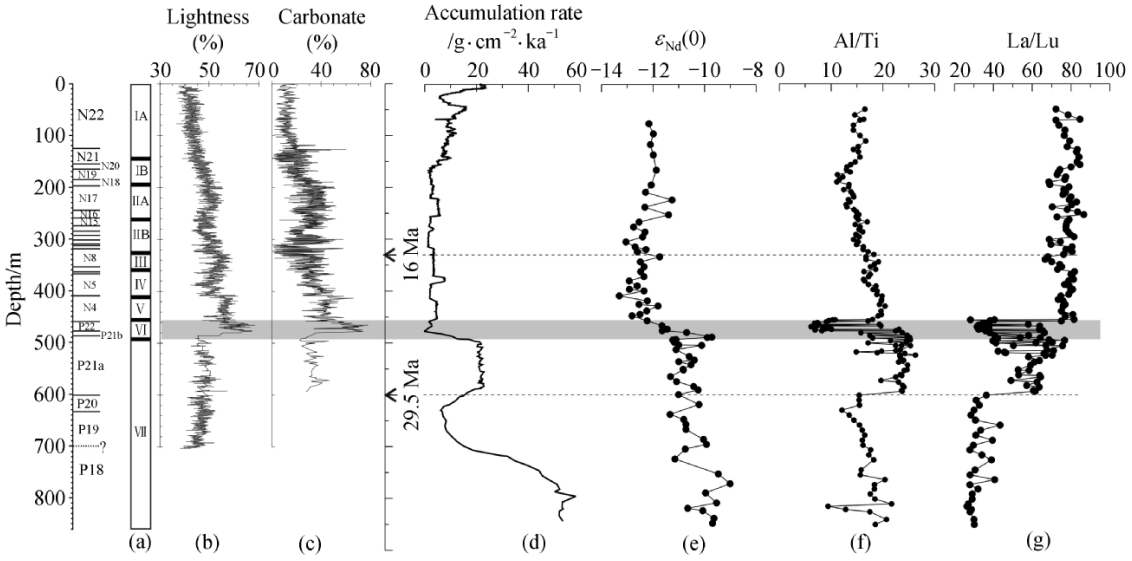

Fig. 6. Stratigraphy, lithology and geochemistry at ODP Site 1148. (a) Lithological units, the Roman denotes unit number, and unit VI is slumping deposits; (b) color reflectance, L*%[5]; (c) $CaCO_3$%[42]; (d) accumulation rate; (e) ε_{Nd}; (f) Al/Ti ratio; (g) La/Lu ratio.

472 m (25.5 Ma to 24.5 Ma), and 460 m (24 Ma to 23.5 Ma). The slumping and unconformities that erased a record of about 3 Ma in total indicate unstable environments caused by frequent tectonic activities in the late Oligocene SCS. These unconformities and poor core recovery (< 20% from 475—510 m and 790—895 m) distort the Oligocene sediment record at this site[4]. Nevertheless, the late Oligocene had been crucial in the SCS development, as all records of physical and chemical logs display an abrupt turn at about 475 m (Fig. 6) that signals a radical reorganization of sedimentary environments and provenance due to tectonics.

(ii) 3.2 Depositional record of seafloor spreading.

Magnetic anomalies reveal three important stages in the early development of the SCS: seafloor spreading began at Chron 11 and ended at Subchron 5c[43], corresponding to the time interval of 30—16.7 Ma using the new palaeomagnetic time scale (or 32—16 Ma on an old time scale)[44,45], and a southward ridge jump occurred at boundary7/6b with an age of 23—25 Ma (old age 24—26 Ma). Since there was no base-rock sampling during Leg 184, direct testing these geophysical results cannot be done. However, the location of Site 1148 at the outer margin of the northern slope is close to the boundary of the continental and oceanic crusts, making the site an ideal place for tracing the spreading history of the SCS basin through the recovered depositional records.

Age and lithostratigraphic analyses indicate that the fast accumulated deposits with turbidites near the base of Site 1148 were related to intense tectonic movements prior to seafloor spreading. At the onset of seafloor spreading about 30 Ma ago, the sedimentation rate decreased at nearly 600 m of Site 1148 (Fig. 7), followed by significant changes in the sedimentary environment characterized by an abrupt increase in the abundance of diatoms and radiolarians in the uppermost lower Oligocene section between 475 m and 600 m (Fig. 5(h), (i))[41]. Seafloor spreading in the SCS differs from the Sea of Japan especially in lacking volcanic activities in the deep water Oligocene. The hemipelagic Oligocene deposits with reworked Eocene marine fossils indicate that a deep-sea basin had already created during early Paleogene rifting well before seafloor

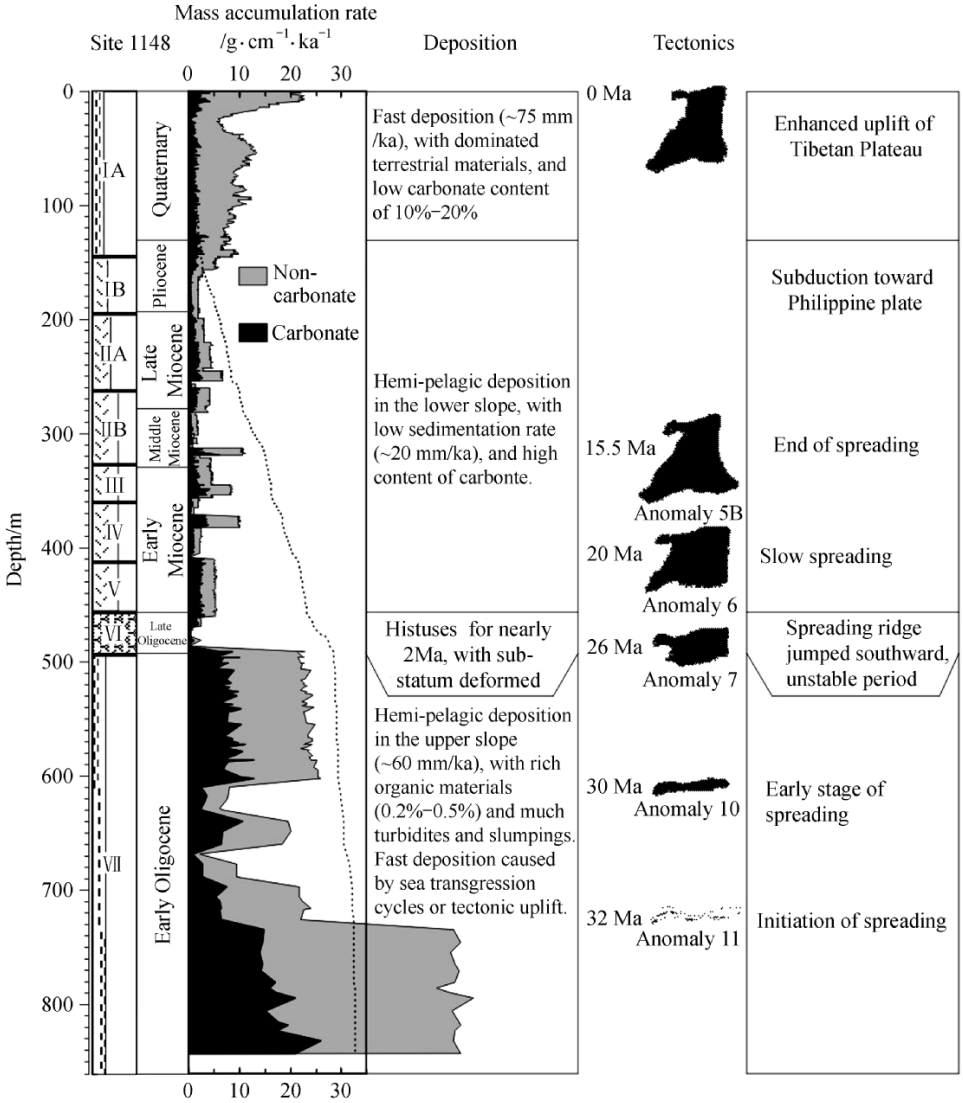

Fig. 7. Seafloor spreading and depositional evolution of the SCS. The accumulation rates modified from [4], the age model for sea floor spreading adjusted according to [43, 44].

spreading actually started 30 Ma ago. The mixture of deep water and nearshore microfossils suggests that the early Oligocene SCS was merely an E-W stretching narrow gulf with steep slopes (Fig. 7).

Following the formation of a deep gulf before 32 Ma and seafloor spreading onset at 30 Ma, the SCS experienced a southward jump of the spreading ridge at 23—25 Ma during the latest Oligocene and earliest Miocene. As noted above, the slumping section at 488—460 m evidences the strongest tectonic influence, shown by the strongest excursions in all logging curves and by the four unconformities that together erased a record of about 3 Ma in the late Oligocene. Geochemical analyses of element concentrations and ratios also reveal a sudden change[46]. The most significant is the decrease in Nd isotope value (ε_{Nd}) from −9 to −11 in the early Oligocene to −12 to −13 in the Miocene (Fig. 6(e)), implying a drastic shift of sources from a southwestern provenance (Indochina-Sunda Shelf and possibly NW Borneo) to a source from the north, i.e. the mainland of China. These geochemical changes are consistent with palaeomagnetic data in indicating the opening up of the E-W stretching gulf and further separation of the southern from the northern slopes of the deep sea basin (Fig. 7). Diagenetic imprints of tectonic influence are found from below the late Oligocene slumping section, with recrystallized foraminiferal tests having most depleted $\delta^{18}O$ values, siliceous fossils transformed from opal-A toward the cristobalite dominated opal-CT[47], and brown-colored fish teeth due to thermal alteration, all markedly different from those younger deposits. Obviously, this 23—25 Ma event represents the strongest tectonic deformation in the basin formation process of the SCS.

After the late Oligocene-earliest Miocene deformation, the SCS basin in the rest of the early Miocene experienced a relatively quiet stage of seafloor spreading with decreased accumulation rates. As a result, lithologic evidence of seafloor spreading became less noticeable but changes in benthic foraminifera and ostracods have revealed rapid increase in water depth and strong carbonate dissolution due to erosive cold water from about 16 Ma (Fig. 6(c)), at about the time seafloor spreading ended[39]. As indicated by ostracod and benthic foraminiferal biofacies, water depth at Site 1148 was about 1500 m in the Oligocene, but deepened to a depth close to the present 3300 m by the end of seafloor spreading. A stable water depth since the later part of the middle Miocene has supported similar benthic assemblages throughout younger time intervals: the late Miocene, Pliocene and Quaternary.

(iii) North-south environmental contrast. Sites 1143 (w.d. 2772 m) and 1146 (w.d. 2092 m) lie on the middle slope of the southern and northern SCS, respectively(see Table 3 in [1]), and provide sediment records for direct comparison of environmental development between the two sectors. Over the past 10 Ma, the carbonate accumulation rate at the northern Site 1146 has been relatively stable, whereas the non-carbonate (terrestrial detritus) content abruptly increased after 3.3 Ma and further increased after 0.4 Ma (Fig. 8(b)). In contrast, both the carbonate and non-carbonate at the southern Site 1143 jumped in the 8.5—6.8 Ma and 6.4—5 Ma periods to almost twice as high as at Site 1146, then declined significantly in the Pliocene, and remained low in younger intervals (Fig. 8(c)). While the high terrestrial flux to the north after 3.3 Ma can be ascribed to continental uplift, intensified weathering and frequent glaciations, the late Miocene high sedimentation rates in the south could have resulted from local tectonic movements, with the tropical Pacific "Biogenic Bloom"[4] influencing local carbonate accumulation. Therefore, Site 1143 in the southern SCS did not show any clear response to uplift of the Tibetan Plateau, while the increase of terrestrial clastics on the northern slope was, at least partly, caused by such global factors as sea level fluctuations due to the growth and decay of boreal ice sheets[48], causing sediment transport from shelves and nearshore into deep sea. Noticeably, the late Miocene $CaCO_3$% at Site 1146 was up to 50%—60% (Fig. 8(b)), which is similar to the modern hemipelagic deposition in the Nansha reef area in the southern SCS. Because the carbonate accumulation rate in the north has not changed significantly over the past 10 Ma, the relatively low fluvial influx until the late Pliocene implies a completely different depositional regime from the post-late Pliocene.

Another aspect of north-south environmental contrast in the evolution of the SCS is thermocline depth variations. As described above, the abundance ratio between planktonic foraminiferal species is closely related to thermocline depth in the upper ocean. When thermocline shoals, the abundance of such mixed layer species as *Globigerinoides ruber*, *Globigerinoides sacculifer* and *Globigerinita glutinata* decrease, whereas those thermocline dwellers such as *Pulleniatina obliquiloculata*, *Globorotalia menardii*, *Globorotalia inflata* and *Neogloboquadrina dutertrei* increase, and vice versa when thermocline deepens[49]. Fig. 9 shows the abundance changes of deep-dwelling planktonic foraminifers since the early Miocene (18 Ma). Until 11.6 Ma, their similar abundance at both Sites 1146 and 1143 indicates a similar thermocline depth between the northern and southern SCS. During the period of 11.5—10.6 Ma, these deep dwelling species developed marked differences: low abundance in the north (minimum 3.5%) and high abundance in the south (maximum 82%). This might indicate a clear gradient in

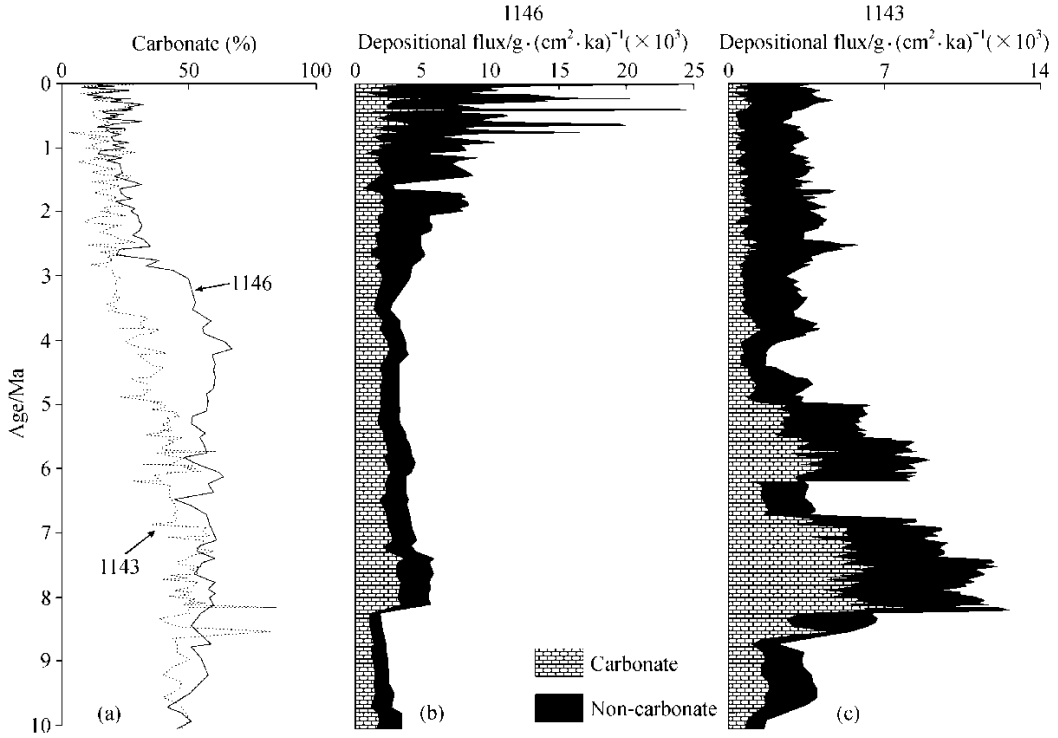

Fig. 8. Comparison of the accumulation rate and sediment composition since 10 Ma between the southern (Site 1143) and northern SCS (Site 1146). (a) $CaCO_3$%, modified from [4]; (b) accumulation rate at Site 1146; (c) accumulation rate at Site 1143, modified from [4].

thermocline depth dipping northward for the first time in the SCS, but the conclusion is hampered by the strong carbonate dissolution, and further work is needed to find out the cause of the changes. A major thermocline deepening with very week fluctuations occurred simultaneously at both sites during 3.6—3.3 Ma before a prominent distinction in their thermocline depth developed. The change in thermocline depth between the southern and northern SCS is believed to have connected to the formation of the Western Pacific Warm Pool (WPWP). The WPWP is characterized by a thick mixed layer with deep thermocline, and its development has had direct impacts on thermocline depth especially the gradient variations between the southern and northern SCS. Therefore, the stable longitudinal gradient after 3.6—3.3 Ma likely marked the formation of the modern-styled WPWP[50].

In summary, the modern environmental pattern with conspicuous N-S contrasts in the SCS has a late Pliocene or even a late Quaternary origin. The N-S contrasts in lithology and thermocline depth described above started nearly 3 Ma ago, compared to the last 1 Ma N-S contrasts in planktonic foraminifer and palynomorph assemblages. *Pulleniatina obliquiloculata* is a warm-water, oligotrophic species often having high abundance in interglacials and low abundance in glacials. After the "Mid-Pleistocene Revolution" about 900 ka ago, however, this species at the southern Site 1143 declined during interglacials or even increased at glacials while its distribution remained "normal" at northern sites, illustrating a prominent late-stage N-S contrast. The late Pleistocene glacial pollen assemblage from the northern SCS contained a large number of herbaceous pollen pointing to an arid environment, whereas the one from the south showed little difference from the humid and warm interglacial assemblage. This again exemplifies late Quaternary N-S contrast in the SCS: climate conditions in the last glaciation were arid in the north but humid in the south[51]. All these phenomena are crucial to the understanding of the evolutionary history of the SCS.

(iv) Environmental significance in basin development. East Asia witnessed a number of events around the Paleogene/Neogene turn: a reversal in topographic relief because of further subduction and uplift in the west, and a reorganization of climate-vegetation zones directly or indirectly influenced by the formation of the Antarctic ice cap. To clarify the time succession of these events and their mutual relationship is the outstanding issue for Earth system sciences of China[52], to which the sedimentary record in the SCS has started making contributions. Although the scientific results summarized above represent a

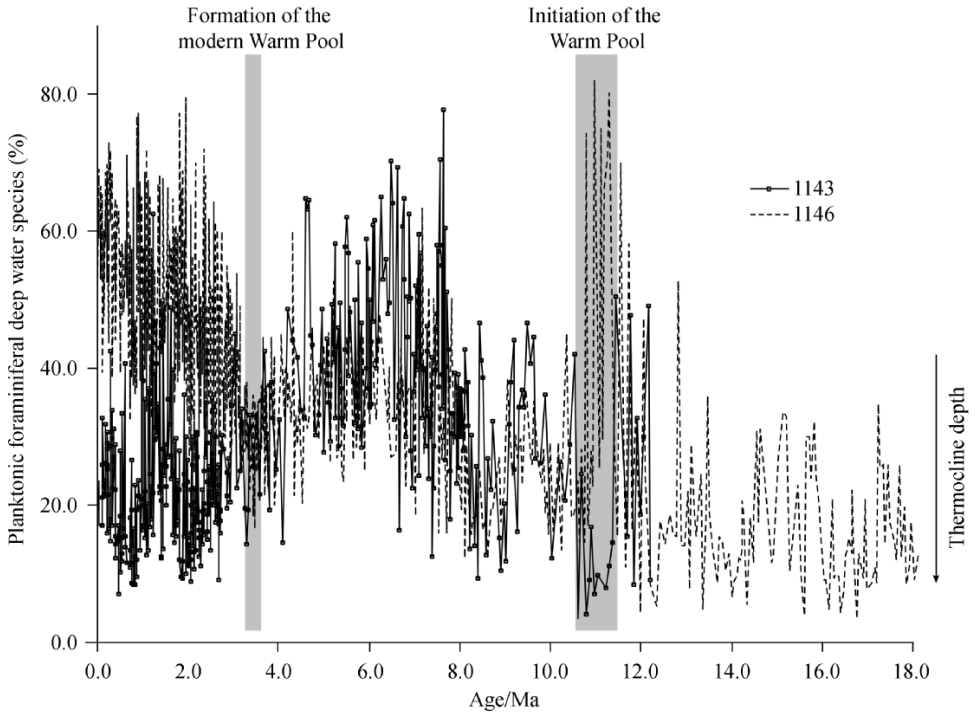

Fig. 9. Downcore variations in percentage of deep dwelling planktonic foraminifers since the Miocene at Sites 1146 and 1143, showing N-S contrasts in the history of thermocline changes in the SCS[50].

small part of progress in ODP Leg 184 studies, they have shown: (1) major environmental changes in East Asia occurred in the late Oligocene but not in the early Miocene, (2) most intensive tectonic activities happened at the end of the late Oligocene when the spreading ridge jumped southward, not at the onset of seafloor spreading (30 Ma); and (3) deep water environments appeared before, not after, seafloor spreading in the SCS.

After the end of seafloor spreading at 15—16 Ma, the SCS's connection with the open ocean started to contract progressively. The closure of the SCS not only enhanced environmental contrasts between the south and the north, but also weakened its exchanges with the Pacific and Indian Oceans, which in turn helped strengthen the WPWP. The SCS records have also improved our understanding of environmental changes on the continental shelf and coastal plains. For example, the pollen record from Site 1144 revealed the broad shelf in the north establishing only 150 ka ago, correlated well with marine transgressions on to shelves and coastal plains since MIS 5. With further studies of the ODP Leg 184 material and further comparing the deep sea results with terrestrial records, more new discoveries on the environmental history of the Western Pacific and China can be predicted.

3 Concluding remarks

The unique geographic feature of the western Pacific is the development of a series of marginal seas between the Earth's largest continent and ocean. The hemipelagic deposits in these marginal seas preserve the richest archive of sea-land interaction history. Over the last 30 years, DSDP and ODP cruises sailed 7 times to the western Pacific[53], including three times to the Sea of Japan and one time to the SCS. Because the Sea of Japan is located at higher latitudes with poor preservation of carbonate and fossils, the SCS cruise has yielded much more abundant environmental information. Moreover, the integration of the SCS record with terrestrial records from China has enabled a new approach to paleo-environmental studies in the region. In addition to the previous summary reports[1,2] describing deep-sea stratigraphic sequences and tropical forcing of climate cycles, this paper summarized the following two major contributions by ODP Leg 184:

(1) Deep-sea records of the East Asian monsoon evolution. The recovered long records revealed a sequence of paleo-climate events especially at 8 Ma, 3.2 Ma, 2.2 Ma and 0.4 Ma. The evolution of the East Asian monsoon was similar to the South Asian monsoon in stages, and the main difference lies in the role of the winter monsoon becoming enhanced over East Asia. In the orbital time scale, the richest spectrum of monsoon records in frequency domain from the southern SCS characterizes the response of low latitudes to insolation forcing. An integration of land and sea data indicates that the East Asian monsoon

can be traced back to more than 20 Ma.

(2) Sedimentary records of the SCS evolution. The recovered sediment sequence by age covers the entire history of seafloor spreading of the SCS basin. The discovery of deep water early Oligocene deposits testifies a deep-sea environment already existed in the early stage of the seafloor spreading. The strongest tectonic deformation occurred in the late Oligocene, at about 25 Ma. The environmental contrast between the north and south SCS started to form only about 3 Ma ago.

The scientific results from ODP Leg 184 have effectively proved the importance of deep sea research and land-sea integration for Earth Science in China. With the inception of the international "Integrated Ocean Drilling Program", China has an obligation to further strengthen its input to deep-sea research and increase its participation in international collaborations.

Acknowledgements This is the third summary report of ODP Leg 184 to the SCS. This work was supported by the National Natural Science Foundation of China (Grant No. 4999560) and the National Key Basic Research Special Foundation (Grant No. G2000078500). This research used samples provided by the Ocean Drilling Program (ODP). ODP is sponsored by the U.S. National Science Foundation (NSF) and participating countries under management of Joint Oceanographic Institutions (JOI), Inc.

References

1. Wang, P., Zhao, Q., Jian, Z. et al., Thirty million year deep-sea records in the South China Sea, Chinese Science Bulletin, 2003, 48(23): 2524—2535.
2. Wang, P., Tian, J., Cheng, X. et al., Exploring cyclic changes of the ocean carbon reservoir, Chinese Science Bulletin, 2003, 48(23): 2536—2548.
3. Prell, W. L., Murray, D. W., Clemens, S. C. et al., Evolution and variability of the Indian Ocean summer monsoon: Evidence from the western Arabian Sea drilling program (ed. Duncan, R. A.), The Indian Ocean: A Synthesis of Results from the Ocean Drilling Program, AGU, Washington, D C, 1992, 447—469.
4. Wang, P., Prell, W., Blum, P. et al., Proceedings of Ocean Drilling Program, Initial Reports, Volume 184, College Station: Ocean Drilling Program, 2000, 77.
5. Sarnthein, M., Pflaumann, U., Wang, P. et al., Preliminary Report on SONNE-95 Cruise "Monitor Monson" to the South China Sea, Reports, Geol-Palaont Inst. Univ. Kiel, 1994, 68: 225.
6. Wang, P., Response of Western Pacific marginal seas to glacial cycles: Paleoceanographic and sedimentological features, Marine Geology, 1999, 156: 5—39.
7. Wang, L., Sarnthein, M., Erlenkeuser, H. et al., East Asian monsoon climate during the Late Pleistocene: High-resolution sediment records from the South China Sea, Marine Geology, 1999, 156: 245—284.
8. Sun, D., Shaw, J., An, Z. et al., Magnetostratigraphy and paleoclimatic interpretation of a continuous 7.2 Ma Late Cenozoic eolian sediments from the Chinese Loess Plateau, Geophysical Research Letters, 1998, 25: 85—88.
9. Ding, Z. L., Sun, J. M., Yang, S. L. et al., Preliminary magnetostratigraphy of a thick eolian red clay-loess sequence at Lingtai, the Chinese Loess Plateau, Geophysical Research Latters, 1998, 25: 1225—1228.
10. An, Z., Kutzbach, J. E., Prell, W. L. et al., Evolution of Asian monsoons and phased uplift of the Himalaya-Tibetan plateau since Late Miocene times, Nature, 2001, 411: 62—66.
11. Guo, Z., Ruddiman, W. F., Hao, Q. Z. et al., Onset of Asian desertification by 22 Ma ago inferred from loess deposits in China, Nature, 2002, 416: 159—163.
12. Zhou, T., Chinese Natural Geography, Paleogeography (1st volume) (in Chinese), Beiing: Science Press, 1984, 262.
13. Wang, P., Neogene stratigraphy and paleoenvironments of China, Palaeo Palaeo Palaeo, 1990, 77: 315—334.
14. Liu, T., Zheng, M., Guo, Z., Initiation and evolution of the Asian monsoon system timely coupled with the ice-sheet growth and the tectonic movements in Asia, Quaternary Sciences (in Chinese), 1998, 3: 194—204.
15. Ducrocq, S., Chaimanee, Y., Suteethorn, V., Ages and paleoenvironment of Miocene mammalian faunas from Thailand, Palaeo Palaeo Palaeo, 1994, 108: 149—163.
16. Ramstein, G., Fluteau, F., Besse, J. et al., Effect of orogeny, plate motion and land-sea distribution on Eurasian climate change over the past 30 million years, Nature, 1997, 386: 788—795.
17. Cheng, L., Liu, J., Zhou, X. et al., Impact of uplift of Tibetan Plateau and change of land-ocean distribution on climate over Asia, Acta Meteorologica Sinica, 2000, 14(4): 450—474.
18. Kroon, D., Darling, K., Size and upwelling control of the stable isotope composition of *Neogloboquadrina dutertrei* (D'Orbigny), *Globigerinoides ruber* (D'Orbigny) and *Globigerina bulloides* D'Orbigny: Examples from the Panama Basin and Arabian Sea, Journal of Foraminiferal Research, 1995, 25: 39—52.
19. Jian, Z., Wang, P., Chen, M. P. et al., Foraminiferal responses to major Pleistocene paleoceanographic changes in the southern South China Sea, Paleoceanography, 2000, 15(2): 229—243.
20. Prell, W., Kutzbach, J., Sensitivity of the Indian monsoon to forcing parameters and implications for its evolution, Nature, 1992, 360: 647—652.
21. Ding, Z. L., Yang, S. L., Hou, S. S. et al., Magnetostratigraphy and sedimentology of Jingchuan red clay section and correlation of the Jinchuan red clay section and correlation of the Tertiary eolian red clay sediments of the Chinese Loess Plateau, Journal of Geophysical Research, 2001, 106: 6399—6407.
22. Molnar, P., England, P., Martiod, J., Mantle dynamics, uplift of the Tibetan Plateau and the Indian monsoon development, Review of Geophysics, 1993, 34: 357—396.
23. Li, J., Wang, R., Li, B., Variations of opal accumulation rates and palaeoproductivity over the past 12 Ma at ODP Site 1143, southern South China Sea, Chinese Science Bulletin, 2002, 47: 596—598.
24. Jian, Z., Wang, P., Zhao, Q. et al., Late Oligocene isotopic and foraminiferal evidences of the intensification of the East Asian monsoon in the northern SCS, Quaternary Sciences (in Chinese), 2001, 21: 461—469.

25. Clemens, S. C., Prell, W., Murray, D. et al., Forcing mechanisms of the Indian Ocean monsoon, Nature, 1991, 353: 720—725.
26. Hilgen, F. J., Extension of the astronomically calibrated (polarity) time scale to the Miocene/Pliocene boundary, Earth and Planetary Science Letters, 1991, 107: 349—368.
27. Wehausen, R., Brumsack, H. J., Tronomical forcing of the East Asian monsoon mirrored by the composition of Pliocene South China Sea sediments, Earth and Planetary Science Letters, 2002, 201: 621—636
28. Wang, P., Tian, J., Cheng, X. et al., Carbon reservoir changes precede major ice-sheets expansion at Mid-Brunhes Event, Geology, 2003, 31: 239—242.
29. Laskar, J., The chaotic motion of the solar system: A numerical estimate of the size of the chaotic zones, Icarus, 1990, 88: 266—291.
30. Chen, P. Y., Minerals in bottom sediments of the South China Sea, Geol. Soc. Am. Bull., 1978, 89: 211—222.
31. Sun, X., Li, X., A pollen record of the last 37 ka in deep sea core 17940 from the northern slope of the South China Sea, Marine Geology, 1999, 156: 227—244.
32. Sun, X., Luo, Y., Deep sea pollen records since 280 ka in the northern SCS, Science in China, Series D, 2001, 44: 879—888.
33. Luo, Y., Chen, H., Wu, G. et al., Records of natural fire and climate history during the last three glacial-interglacial cycles around the South China Sea—Charcoal record from the ODP 1144, Science in China, Series D, 2001, 44: 897—904.
34. Liu, C., Cheng, X., Exploring variations in upper ocean structure for the last 2 Ma of the Nansha area by means of calcareous nannofossils, Science in China, Series D, 2001, 44: 905—911.
35. Wang, R., Li, J., Quaternary high resolution opal record and its paleoproductivity, Chinese Science Bulletin, 2003, 4: 363—367.
36. Pak, D. K., Kennett, J. P., A foraminiferal isotopic proxy for upper water mass stratification, Journal of Foraminiferal Research, 2002, 32: 319—327.
37. Short, D. A., Mengel, J. G., Crowley, T. J. et al., North GR. Filtering of Milankovitch cycles by Earth's geography, Quaternary Research, 1991, 35: 157—173
38. Chen Longxun, East Asian Monsoon (in Chinese), Beijing: Meteonolgical Press, 1991. 362.
39. Kuhnt, W., Holbourn, A., Zhao, Q., The early history of the South China Sea: Evolution of Oligocene-Mioecne deep water environments, Revue de Micropaleontologie, 2002, 45: 99—159.
40. Haq, B. U., Hardenbol, J., Vail, P. R., Chronology of fluctuating sea levels since the Triassic (250 million years ago to present), Science, 1987, 235: 1156—1167.
41. Wang, R., Fang, D., Shao, L. et al., Oligocene biogenic siliceous deposits on the slope of the northern South China Sea, Science in China, Series D, 2001, 44: 912—918.
42. Chen, X., Zhao, Q., Jian, Z., Carbonate content changes since the Miocene and paleoenvironmental implications, ODP Ssite 1148, northern South China Sea. Marine Geology and Quaternary Geology (in Chinese with English abstract), 2002, 22(2): 69—74.
43. Briais, A., Patriat, P., Tapponnier, P., Updated interpretation of magnetic anomalies and seafloor spreading stages in the South China Sea: Implications for the Tertiary tectonics of Southeast Asia, Journal of Geophysical Research, 1993, 98(B4): 6299—6328.
44. Cande, S. C., Kent, D. V., A new geomagnetic polarity time scale for the late Cretaceous and Cenozoic, J. Geophys. Res., 1992, 97: 13917—13951.
45. Berggren, W. A., Kent, D. V., Swisher, III. C. C. et al., A revised Cenozoic geochronology and chronostratigraphy (eds. Berggren, W. A. et al.), Geochronology, Time Scales and Global Stratigraphic Correlation, Spec. Publ. SEPM 54, 1995, 129—212.
46. Li, X. H., Wei, G., Shao, L. et al., Geochemical and Nd isotopic variations in sediments of the South China Sea: a response to Cenozoic tectonism in SE Asia, Earth and Planetary Science Letters, 2003, 211: 207—220.
47. Fang, D., Wang, R., Shao, L. et al., Silica diagenesis of dep-sea Oligocene at ODP Site 1148, the South China Sea, Marine Geology and Quaternary Geology (in Chinese with English abstract), 2002, 22(2): 75—79.
48. Zhang, P. Z., Peter, M., William, R. D., Increased sedimentation rates and grain size 2—4 Ma ago due to the influence of climate change on erosion rates, Nature, 2001, 410: 891—897.
49. Ravelo, A. C., Fairbanks, R. G., Philander, S. G., Reconstruction tropical Atlantic hydrography using planktonic foraminifera and an ocean model, Paleoceanography, 1990, 5(3): 409—431.
50. Jian, Z., Li, B., Wang, J., Formation and evolution of the Western Pacific Warm Pool recorded by microfossils, Quaternary Sciences (in Chinese with English abstract), 2003, 23: 185—192.
51. Sun, X., Li, X., Lou, Y. et al., The vegetation and climate at the last glaciation on the emerged continental shelf of the South China Sea, Palaeo Palaeo Palaeo, 2000, 160: 301—316.
52. Wang Pinxian, Deformation of Asia and global cooling: searching links between climate and tectonics, Quaternary Sciences (in Chinese with English abstract), 1998, 3: 213—221.
53. Jin, X., Zhou, Z., Wang, P., Ocean Drilling Program and Earth Sciences in China (in Chinese), Shanghai: Tongji University Press, 1995, 349.

(Received April 1, 2003; accepted July 28, 2003)